# Spin relaxation dynamics with a continuous spin environment: The dissipaton equation of motion approach



Special Collection: Algorithms and Software for Open Quantum System Dynamics

Wenxiang Ying 🗷 📵 ; Yu Su 📵 ; Zi-Hao Chen 📵 ; Yao Wang 📵 ; Pengfei Huo 📵



J. Chem. Phys. 161, 144112 (2024) https://doi.org/10.1063/5.0225734





### Articles You May Be Interested In

Open quantum systems with nonlinear environmental backactions: Extended dissipaton theory vs coresystem hierarchy construction

J. Chem. Phys. (February 2023)

Equilibrium and transient thermodynamics: A unified dissipaton-space approach

J. Chem. Phys. (October 2020)

Entangled system-and-environment dynamics: Phase-space dissipaton theory

J. Chem. Phys. (January 2020)

# Challenge us.

What are your needs for periodic signal detection?



Find out more





## Spin relaxation dynamics with a continuous spin environment: The dissipaton equation of motion approach

Cite as: J. Chem. Phys. 161, 144112 (2024); doi: 10.1063/5.0225734 Submitted: 26 June 2024 · Accepted: 19 September 2024 ·









**Published Online: 10 October 2024** 













- Department of Chemistry, University of Rochester, 120 Trustee Road, Rochester, New York 14627, USA
- <sup>2</sup>Department of Chemical Physics, University of Science and Technology of China, Hefei, Anhui 230026, China
- <sup>3</sup>Department of Chemistry, The University of Hong Kong, Pokfulam Road, Hong Kong, China
- <sup>4</sup>The Institute of Optics, Hajim School of Engineering, University of Rochester, Rochester, New York 14627, USA

Note: This paper is part of the JCP Special Topic on Algorithms and Software for Open Quantum System Dynamics.

- <sup>a)</sup>Author to whom correspondence should be addressed: wying3@ur.rochester.edu
- b) Electronic mail: wy2010@ustc.edu.cn
- c) Electronic mail: pengfei.huo@rochester.edu

### **ABSTRACT**

We investigate the quantum dynamics of a spin coupling to a bath of independent spins via the dissipaton equation of motion (DEOM) approach. The bath, characterized by a continuous spectral density function, is composed of spins that are independent level systems described by the su(2) Lie algebra, representing an environment with a large magnitude of anharmonicity. Based on the previous work by Suarez and Silbey [J. Chem. Phys. 95, 9115 (1991)] and by Makri [J. Chem. Phys. 111, 6164 (1999)] that the spin bath can be mapped to a Gaussian environment under its linear response limit, we use the time-domain Prony fitting decomposition scheme to the bare-bath time correlation function (TCF) given by the bosonic fluctuation-dissipation theorem to generate the exponential decay basis (or pseudo modes) for DEOM construction. The accuracy and efficiency of this strategy have been explored by a variety of numerical results. We envision that this work provides new insights into extending the hierarchical equations of motion and DEOM approach to certain types of anharmonic environments with arbitrary TCF or spectral density.

Published under an exclusive license by AIP Publishing. https://doi.org/10.1063/5.0225734

### I. INTRODUCTION

The dynamics of a two-level system (TLS) coupling to a dissipative environment have been extensively investigated over the past decades. The most widely and systematically studied one is the spin-boson model, 1-4 which has various applications in physics and chemical dynamics in condensed phase. 1-6 The environmental part of the spin-boson model is a set of non-interacting harmonic oscillators. This is reasonable as Caldeira and Leggett<sup>7</sup> had justified the universality of bosonic heat baths consisting of an infinite number of harmonic oscillators that are linearly coupled to the system.

Apart from the bosonic environment, another typical environment of interest is a bath consisting of a set of spins, 8,9 which can be regarded as an extreme example of an anharmonic environment. The spin-spin-bath (SSB) model denotes a TLS coupled with a dissipative spin bath. It has recently drawn tremendous attention due to interesting phenomena in physical setups. For example, it is predicted and justified that at very low temperature, the dynamics of magnetic nanoclusters, such as Fe<sub>8</sub> and Mn<sub>12</sub>, is strongly influenced by nuclear spins; 10-14 for solid-state quantum computing devices whose qubits are typically electron spins, such as GaAs quantum dot<sup>15-17</sup> and diamonds with nitrogen-vacancy (NV) centers, <sup>18,19</sup> it is inevitable for the qubits to be coupled to environmental spins. The spin environment is also concerned in stylized quantum measurement setups, <sup>20,21</sup> the studies of quantum phase transition, <sup>17,22,23</sup> and more recently, the radical pair spin relaxation as well as its applications in quantum information processing.<sup>24–27</sup> Being anharmonic but very simple (in terms of Hamiltonian), the SSB model provides new insights into quantum dynamics in the condensed

The theoretical treatment of the anharmonic spin bath has been discussed by Suarez and Silbey,<sup>28</sup> Makri,<sup>29</sup> and later by Yan et al.<sup>30</sup> They proved that under the thermodynamics limit (also known as the linear response limit), the generally anharmonic spin bath approximately satisfies the Gaussian statistics, despite that Ref. 28 did not prove the harmonic bath mapping except only for the special case of pure dephasing, which is analytically treatable. As a result, the spin bath can be effectively characterized by the familiar boson bath with a modified spectral density function, which is much easier to treat by using a wide range of quantum dynamics methods. On this basis, higher-order nonlinear effects can be further studied by considering a finite number of bath spins. Previous work on the quantum dynamics of SSB types of models have been carried out extensively by using the iterative path integral approach based on influence functional, <sup>29,31,32</sup> the multilayer multiconfiguration time-dependent Hartree (ML-MCTDH)<sup>33</sup> and the closely related surrogate Hamiltonian<sup>34,35</sup> approach, polaron-transformed master equation,<sup>36</sup> Nakajima-Zwanzig type of generalized master equation,<sup>37</sup> and the generalized hierarchical equations of motion (gHEOM) that is based on the stochastic Liouville equation with perturbative expansion scheme.<sup>38,3</sup>

A variety of approximation-based methods are also developed and applied for the spin bath problems, such as the time-dependent perturbation approach, 40 phase space quasi-classical methods. 41 A number of cluster expansion (CE) approaches,<sup>42</sup> including the cluster correlation expansion, 43-45 linked cluster expansion, 46 and the associated dynamical mean field theory,<sup>47</sup> have been developed to study the many-body bath time evolution. Nakamura and Tanimura<sup>48</sup> studied the dynamics of a TLS that interacts with a subenvironment consisting of a one-dimensional XXZ spin chain using the hierarchical Schrödinger equations of motion (HSEOM), despite that the noise generated from the spin-lattice is non-Gaussian and non-local, and the spin chain environment is entirely different from the TLS bath. It should be noted that the independent TLS bath is rather trivial through harmonic mapping, while spin chains are very challenging. <sup>2,49</sup> The series of work done by Fay, Lindoy, and Manolopoulos <sup>24,25,50-53</sup> had provided a systematic theoretical framework for electron spin relaxation in radical pairs that exposed to an environment of nuclear spins, which includes full quantum mechanical treatment of all spin degrees of freedom using tensor network propagation strategy and master equation approaches based on the Schulten-Wolvnes semiclassical treatment to the nuclear spins. It should be noted that for many problems in electron paramagnetic resonance (EPR)/radical pair spin dynamics, where the spin bath is large but finite, the spin-to-boson map is not valid because the linear response is not rigorously reached. As a result, one would need to use the MCTDH and its multilayer extension, the path integralbased approaches, or approximated approaches, such as perturbative master equations and trajectory-based methods, which can deal with discrete and finite spin modes. On the other hand, if the spin bath is indeed very large, then one could assume the thermodynamics limit and use a continuous function to fit the spectral density, so that the spin-to-boson map can still be adopted, being a good

Despite the fruitful progress, all these approaches have their specific limitations. For example, increasing the memory length will usually lead to less efficient propagation for the direct path integralbased method. The recently developed SMaPI algorithm <sup>54,55</sup> further

facilitated the long-memory calculations by eliminating the tensor storage of the original path integral algorithm;<sup>56–58</sup> the numerically exact ML-MCTDH approach, which relies on a discretization strategy for the continuous bath spectral density, is computational costly to reach numerical convergence for models with high bath cutoff frequency so that Born-Oppenheimer (BO) type of approximation needs to be made; 1,33 MCTDH is more computational demanding under the finite-temperature case due to its dependence on the Monte Carlo sampling strategy.<sup>59</sup> Furthermore, almost all the work mentioned above only takes care of the spin-1/2 case. In realistic situations, however, the nuclear spin quantum numbers are usually much larger than 1/2.

Regarding the limitations of current studies on the spin bath mentioned above, a more general, numerically efficient, and accurate theoretical framework needs to be developed. The dissipaton equation of motion (DEOM) is a statistical quasi-particle theory for quantum dissipative dynamics. Featured by the very powerful dissipaton algebras, it not only just recovers HEOM formalism<sup>60–62</sup> but also identifies the physical meanings of the dynamical variables. 9,63 Equipped with the time-domain Prony fitting decomposition  $(t\text{-PFD})^{64}$  scheme, by which the environmental time correlation function (TCF) can be accurately decomposed into exponential sums, the efficiency and applicability of HEOM/DEOM is significantly improved. Notably, the t-PFD scheme is, in principle, applicable to arbitrary bath TCF or spectral density. Under the linear response limit, the theory of effective spectral density function provides a perfect platform for us to play with t-PFD.

In this work, by taking advantage of the linear response limit, we generalize the theory of effective spectral density function for spin bath with arbitrary bath spin quantum number S. Then, we apply DEOM to study the spin relaxation dynamics of a TLS coupling to the effective bosonic environment. The bath TCF decomposition is achieved by t-PFD. This paper is organized as follows: in Sec. II, we briefly review the spin bath model, its linear response properties, bosonic DEOM, and t-PFD scheme; in Sec. III, we present various numerical testing results for SSB models, including zero- and finite-temperature, weak and strong coupling, unbiased and biased cases with comparisons against ML-MCTDH; in Sec. IV, we briefly summarized the major advantage of our method.

### II. MODEL AND METHODOLOGY

The total TLS-plus-bath composite Hamiltonian of an open quantum system reads as

$$\hat{H} = \hat{H}_S + \hat{h}_B + \hat{H}_{SB},\tag{1}$$

where  $\hat{H}_S \equiv \epsilon \hat{\sigma}_z + \Delta \hat{\sigma}_x$  is the system Hamiltonian of a TLS with energy bias  $\epsilon$  and off-diagonal coupling  $\Delta$ . Furthermore,  $\hat{\boldsymbol{\sigma}} \equiv (\hat{\sigma}_x, \hat{\sigma}_y, \hat{\sigma}_z)$  denotes the Pauli matrices;  $\hat{h}_B$  is the bath Hamiltonian that usually consists of a macroscopic number of noninteracting particles that can be bosons, fermions, and/or spins. In addition,  $\hat{H}_{SB}$  carries the system-bath interaction. The influence of the bath entails quantum statistical mechanics description, in which the thermodynamics limit is naturally assumed. We set  $\hbar \equiv 1$  throughout this paper for the sake of convenience.

#### A. The spin bath models

The spin bath and its interaction with the system can be described by the Hamiltonian in the following: <sup>29,33,39</sup>

$$\hat{h}_{\rm B} = \sum_{j=1}^{N} \omega_j \hat{s}_z^j, \tag{2a}$$

$$\hat{H}_{SB} = \sum_{a} \hat{Q}_{a} \otimes \hat{F}_{a}. \tag{2b}$$

The bath Hamiltonian  $\hat{h}_B$  describes N independent spins, which are distinguishable. It is diagonal in the  $\{(\hat{\mathbf{s}}^j)^2, \hat{\mathbf{s}}_z^j \mid j=1,\ldots,N\}$  eigen representation, where  $\hat{\mathbf{s}}^j$  are the spin operators associated with the jth bath mode, characterized by energy difference  $\omega_j$ . They form the  $\bigotimes_{j=1}^N \mathfrak{su}(2)$  Lie algebra,  $[\hat{\mathbf{s}}_\alpha^i, \hat{\mathbf{s}}_\beta^j] = i\delta_{ij}\epsilon_{\alpha\beta\gamma}\hat{\mathbf{s}}_\gamma^i$ , where  $\alpha, \beta, \gamma$  denote the Cartesian components of the spin matrices,  $\epsilon_{\alpha\beta\gamma}$  is the 3-D Levi–Cività tensor, and  $\delta_{ij}$  is the Kronecker symbol. Finally,  $\{\hat{Q}_a\}$  and  $\{\hat{F}_a\}$  denote the system and bath dissipation modes, respectively.

There are extensive types of spin–spin interaction, such as the Ising type<sup>65</sup> and the Heisenberg type,<sup>66</sup> whose general expression takes the form  $\hat{\sigma}_{\alpha}\hat{s}^{j}_{\beta}$ . Among the various choices, the most common types can be summarized as<sup>39</sup>

$$\hat{H}_{SB} = \begin{cases} \frac{1}{\sqrt{S}} \sum_{j=1}^{N} c_{j} \hat{s}_{x}^{j} \hat{\sigma}_{z}, \\ \frac{1}{\sqrt{S}} \sum_{j=1}^{N} c_{j} \hat{s}_{z}^{j} \hat{\sigma}_{z}, \\ \frac{1}{\sqrt{S}} \sum_{j=1}^{N} c_{j} (\hat{s}_{x}^{j} \hat{\sigma}_{x} + \hat{s}_{y}^{j} \hat{\sigma}_{y}), \\ \frac{1}{\sqrt{S}} \sum_{j=1}^{N} c_{j} (\hat{s}_{x}^{j} \hat{\sigma}_{x} + \hat{s}_{y}^{j} \hat{\sigma}_{y} + \hat{s}_{z}^{j} \hat{\sigma}_{z}), \end{cases}$$
(3)

where  $c_j$  are the coupling coefficients between the system dissipation operators and the jth bath mode, and S is the spin quantum number of the bath spins. In this paper, we focus on the first interaction form in Eq. (3). According to Caldeira and Leggett, <sup>7</sup> the bath and its coupling to the system might be described by the spectral density function, defined as

$$J_{ab}(\omega) \equiv \frac{\pi}{2} \sum_{i=1}^{N} c_{aj}^{*} c_{bj} \delta(\omega - \omega_{j}), \tag{4}$$

where the coupling coefficients are assumed to obey the general scaling rule,  $c_{aj} \sim 1/\sqrt{N}$ .

It is worth noting that the spin bath is not generally a Gaussian environment. Suarez and Silbey<sup>28</sup> as well as Makri<sup>31</sup> have remarkably shown that under the limit of  $N \to +\infty$ , the SSB model with bath spin quantum number S = 1/2, can be rigorously mapped onto the familiar spin-boson model with an effective spectral density,

$$[J_{ab}]_{\text{eff}}(\omega;\beta) = J_{ab}(\omega) \tanh(\beta\omega/2), \tag{5}$$

with the subscript a=b for the single mode case. More specifically, only the second-order term remains in the cumulant expansion of the influence functional under the  $N \to +\infty$  limit. The higher order cumulants  $\mathcal{O}(1/\sqrt{N})$  will disappear under the scaling limit. As a

result, the noise spectra of the bath dissipation operators are Gaussians,  $^{28}$  leading to the linear response limit. The effective boson bath spectral density is derived based on re-expressing the spin bath TCF as the boson bath TCF multiplied by the  $\tanh(\beta\omega/2)$  factor.  $^{31}$  There is a straightforward example with respect to the pure dephasing case, in which  $\Delta=0$  such that the dephasing dynamics has an analytical solution, as discussed by Rao and Kurizki  $^{67}$  as well as Hsieh and Cao.  $^{39}$ 

### B. Linear response of the spin bath and generalized theory of the effective spectral density function

As is discussed above, the continuous spin bath approximately satisfies Gaussian statistics. The influence of Gaussian environments is completely characterized by the linear response functions of hybrid bath modes in the isolated bare–bath subspace. For the bosonic environment, it can be defined via the commutator as

$$\chi_{ab}(t) \equiv i\langle [\hat{F}_a(t), \hat{F}_b(0)] \rangle_{\mathcal{B}}. \tag{6}$$

Here,  $\hat{F}(t) = e^{i\hat{h}_B t} \hat{F}(0) e^{-i\hat{h}_B t}$  exerts the *stochastic force*, and  $\langle (\cdot) \rangle_B \equiv \operatorname{tr}_B[(\cdot) \rho_B^{eq}(T)]$  denotes the ensemble average in the bath subspace, with  $\rho_B^{eq}(T) \equiv e^{-\beta \hat{h}_B} / \operatorname{tr}_B[e^{-\beta \hat{h}_B}]$ . For fermionic environments, the similar concept can also be defined via the anti-commutator, <sup>2,9</sup>

$$G_{ab}(t) \equiv \langle \{\hat{F}_a(t), \hat{F}_b(0)\} \rangle_{\mathcal{B}},\tag{7}$$

which is known as the single-particle Green's function. The *causality* Fourier transform of  $\chi_{ab}(t)$  and  $G_{ab}(t)$  is defined as

$$\chi_{ab}(\omega) \equiv \int_0^\infty dt \ e^{i\omega t} i\langle [\hat{F}_a(t), \hat{F}_b(0)] \rangle_{\rm B},$$
(8a)

$$G_{ab}(\omega) \equiv \int_0^\infty dt \ e^{i\omega t} \langle \{\hat{F}_a(t), \hat{F}_b(0)\} \rangle_{\text{B}}. \tag{8b}$$

One can easily check their symmetry (being even or odd functions for real and imaginary parts). The spectral density functions can be evaluated using time-reversal symmetry (TRS) as<sup>2</sup>

$$J_{ab}(\omega) = \frac{1}{2i} [\chi_{ab}(\omega) - \chi_{ba}^*(\omega)]$$
$$= \frac{1}{2} \int_{-\infty}^{+\infty} dt \ e^{i\omega t} \langle [\hat{F}_a(t), \hat{F}_b(0)] \rangle_{B}, \tag{9a}$$

$$J'_{ab}(\omega) = \frac{1}{2} \left[ G_{ab}(\omega) + G^*_{ba}(\omega) \right]$$
$$= \frac{1}{2} \int_{-\infty}^{+\infty} dt \ e^{i\omega t} \langle \{ \hat{F}_a(t), \hat{F}_b(0) \} \rangle_{\mathbf{B}}, \tag{9b}$$

corresponding to the bosonic and fermionic cases, respectively. Similarly, one can define the TCF and its spectrum functions as

$$C_{ab}(t) \equiv \langle \hat{F}_a(t)\hat{F}_b(0)\rangle_{\rm B},$$
 (10a)

$$C_{ab}(\omega) \equiv \int_0^\infty dt \ e^{i\omega t} \langle \hat{F}_a(t) \hat{F}_b(0) \rangle_{\rm B}.$$
 (10b)

Without loss of generality, we consider the case of linear system-bath coupling with only one dissipation mode,

$$\hat{F} = \frac{1}{\sqrt{S}} \sum_{j} c_j \hat{s}_x^j, \tag{11}$$

for the spin bath with S = 1/2. Here, we drop all the subscripts for simplicity. One will finally arrive at its FDT with respect to the auto-TCF of the bath dissipation operator,

$$C(t) = \frac{1}{\pi} \int_{-\infty}^{+\infty} d\omega \frac{e^{-i\omega t} J'(\omega)}{1 + e^{-\beta \omega}},$$
 (12)

and detailed derivations are provided in Appendix A. On the other hand, one can independently obtain that

$$C(t) = \frac{1}{\pi} \int_{-\infty}^{+\infty} d\omega \, \frac{e^{-i\omega t} J_{\text{eff}}(\omega; \beta)}{1 - e^{-\beta \omega}},\tag{13}$$

where  $J_{\rm eff}(\omega; \beta) \equiv J(\omega) = J'(\omega) \tanh(\beta \omega/2)$ , recovering Eq. (5), the well-known result. Very interestingly, the continuous spin environment is isomorphic to a boson environment with a temperature-dependent effective spectral density function, whose zero-temperature limit gives rise to  $J'(\omega) = J(\omega)$ . For this reason, the zero-temperature spin-boson model is also widely known as *taking the spin-bath limit*. <sup>68</sup> Despite this being a well-known result, the derivation procedure we outlined here is new.

Due to the generality of the linear response limit, the theory of effective spectral density is widely applicable, so that it is not restricted to S = 1/2 case, but to arbitrary S, as long as the system-bath coupling is linear. We also provide discussions upon arbitrary spin S case in Appendix A, which can be viewed as a generalization of the effective spectral density function theory. This result, summarized in Eq. (A22) is a straightforward generalization for S = 1/2 case. To the best of our knowledge, it is new despite it being well expected.

#### C. Bosonic DEOM formalism

Based on the previous discussion, the open quantum system problem with a continuous spin environment will be exactly mapped to the familiar spin-boson type of model with an effective spectral density function, which has the Hamiltonian description as given in the following:

$$\hat{H} = \hat{H}_{S} + \frac{1}{2} \sum_{j} \omega_{j} (\hat{x}_{j}^{2} + \hat{p}_{j}^{2}) + \sum_{a} \hat{Q}_{a} \otimes \sum_{j} c'_{aj} \hat{x}_{aj}, \qquad (14)$$

where  $\hat{x}_j$  and  $\hat{p}_j$  are the conjugated coordinate-momentum pairs that satisfy the Heisenberg commutation relations,  $\{\hat{Q}_a\}$  are the original system dissipation mode, and  $\{c'_{aj}\}$  are the rescaled coupling coefficients due to the effective spectral density. The problem is now readily to be solved by HEOM/DEOM.

The DEOM theory is a statistical quasi-particle theory for quantum dissipative dynamics, describing the influence of bulk environments using only a few numbers of quasi-particles, the dissipatons. <sup>9,63</sup> They arise strictly from the linear bath coupling component,

$$\hat{F}_a = \sum_{k=1}^K \hat{f}_{ak},\tag{15}$$

with single-damping parameters given by

$$\langle \hat{f}_{ak}(t)\hat{f}_{bj}(0)\rangle_{\rm B} = \delta_{kj}\eta_{abk}e^{-\gamma_{ak}t},$$
 (16a)

$$\langle \hat{f}_{bj}(0)\hat{f}_{ak}(t)\rangle_{\mathcal{B}} = \delta_{kj}\eta_{ab\bar{k}}^* e^{-\gamma_{ak}t}.$$
 (16b)

The associated index  $\bar{k}$  in Eq. (16b) is defined as  $\gamma_{a\bar{k}} = \gamma_{ak}^*$  to preserve TRS. Further denote

$$\langle \hat{f}_{ak} \hat{f}_{bj} \rangle_{\mathbf{B}}^{>} \equiv \langle \hat{f}_{ak} (0^{+}) \hat{f}_{bj} (0) \rangle_{\mathbf{B}} = \delta_{kj} \eta_{abk}, \tag{17a}$$

$$\langle \hat{f}_{bj} \hat{f}_{ak} \rangle_{\mathbf{B}}^{<} \equiv \langle \hat{f}_{bj}(0) \hat{f}_{ak}(0^{+}) \rangle_{\mathbf{B}} = \delta_{kj} \eta_{ab\bar{k}}^{*}, \tag{17b}$$

for later use in the dissipaton algebra. It should be noted that they are different from  $\langle \hat{f}_{ak} \hat{f}_{bj} \rangle_{\text{B}}$ . Equations (15) and (16) leads to

$$\langle \hat{F}_a(t)\hat{F}_b(0)\rangle_{\mathcal{B}} = \sum_{k=1}^K \eta_{abk} e^{-\gamma_{ak}t},\tag{18}$$

and its complex conjugation.

The dynamical variables in DEOM are the dissipaton density operators (DDOs),

$$\rho_{\mathbf{n}}^{(n)}(t) \equiv \mathrm{Tr}_{\mathbf{B}} \left[ \left( \prod_{ak} \hat{f}_{ak}^{n_{ak}} \right)^{\circ} \rho_{\mathbf{T}}(t) \right], \tag{19}$$

where  $\rho_{\rm T}(t)$  is the time-dependent total density matrix, the product of dissipatons inside  $(\cdots)^\circ$  means *irreducible*. In addition, (c-number) $^\circ=0$ . Bosonic dissipatons are symmetric under the permutation,  $(\hat{f}_{ak}\hat{f}_{bj})^\circ=(\hat{f}_{bj}\hat{f}_{ak})^\circ$ . Each DDO in Eq. (19) represents a specific configuration of  $\mathbf{n} = \{\cdots, n_{ak}, \cdots | a=1, \ldots, M; k=1,\ldots,K\}$ , with  $n=\sum_{ak}n_{ak}$  dissipatons in total (*i.e.*, the number of tiers). We also denote that the associated DDO's index  $\mathbf{n}_{ak}^\pm$  differs from  $\mathbf{n}$  at the specified  $n_{ak}$  by  $\pm 1$ , which means  $n_{ak}$  is replaced by  $n_{ak} \pm 1$ .

The DEOM formalism can be constructed according to the dissipaton algebra, which includes the *generalized diffusion equation* and *generalized Wick's theorem*. The generalized diffusion equation arises from the single-damping character in Eq. (16), that

$$\operatorname{Tr}_{B}\left[\left(\frac{\partial \hat{f}_{ak}}{\partial t}\right)_{B} \rho_{T}(t)\right] = -\gamma_{ak} \operatorname{Tr}_{B}\left[\hat{f}_{ak} \rho_{T}(t)\right]. \tag{20}$$

The generalized diffusion equation is applicable for the  $\hat{h}_{\rm B}$ -action,

$$\rho_{\mathbf{n}}^{(n)}(t; h_{\mathrm{B}}^{\times}) \equiv \mathrm{Tr}_{\mathrm{B}} \left\{ \left( \prod_{ak} \hat{f}_{ak}^{n_{ak}} \right)^{\circ} [\hat{h}_{\mathrm{B}}, \rho_{\mathrm{T}}(t)] \right\}$$

$$= \mathrm{Tr}_{\mathrm{B}} \left\{ \left[ \left( \prod_{ak} \hat{f}_{ak}^{n_{ak}} \right)^{\circ}, \hat{h}_{\mathrm{B}} \right] \rho_{\mathrm{T}}(t) \right\}$$

$$= -i \left( \sum_{ak} n_{ak} \gamma_{ak} \right) \rho_{\mathbf{n}}^{(n)}(t), \tag{21}$$

where  $h_{\rm B}^{\times} = [\hat{h}_{\rm B}, \cdot]$ , the second line of Eq. (21) arises from the equivalence between the Schrödinger and Heisenberg prescription, and the last line goes with Heisenberg equations of motion,  $(\partial \hat{f}_{ak}/\partial t)_{\rm B} = -i[\hat{f}_{ak},\hat{h}_{\rm B}]$ . Equation (21) summarizes the contribution by the bath Hamiltonian to the DDOs dynamics. <sup>9,63</sup>

Generalized Wick's theorem deals with the system-hybrid-bath interaction, reading as

$$\operatorname{Tr}_{B}\left[\left(\prod_{ak}\hat{f}_{ak}^{n_{ak}}\right)^{\circ}\hat{f}_{bj}\rho_{T}(t)\right] = \rho_{\mathbf{n}_{bj}^{+}}^{(n+1)}(t) + \sum_{ak}n_{ak}\left(\hat{f}_{ak}\hat{f}_{bj}\right)^{>}{}_{B}\rho_{\mathbf{n}_{ak}^{-}}^{(n-1)}(t),$$
(22a)

$$\operatorname{Tr}_{B}\left[\left(\prod_{ak} \hat{f}_{ak}^{n_{ak}}\right)^{\circ} \rho_{T}(t) \hat{f}_{bj}\right] = \rho_{\mathbf{n}_{bj}^{+}}^{(n+1)}(t) + \sum_{ak} n_{ak} (\hat{f}_{ak} \hat{f}_{bj})^{<}_{B} \rho_{\mathbf{n}_{ak}^{-}}^{(n-1)}(t).$$
(22b)

They will be used in evaluating the commutator action of linear system–bath coupling terms. The bosonic DEOM formalism is now readily to be constructed, reading as <sup>9,63</sup>

$$\dot{\rho}_{\mathbf{n}}^{(n)}(t) = -\left(i\mathcal{L}_{S} + \sum_{ak} n_{ak} \gamma_{ak}\right) \rho_{\mathbf{n}}^{(n)}(t) - i\sum_{ak} \mathcal{Q}_{a}^{\times} \rho_{\mathbf{n}_{ak}^{+}}^{(n+1)}(t) - i\sum_{abk} n_{ak} (\gamma'_{abk} \mathcal{Q}_{b}^{\times} + i\gamma''_{abk} \mathcal{Q}_{b}^{\circ}) \rho^{(n-1)}_{\mathbf{n}_{ak}^{-}}(t).$$
(23)

The involved superoperators and coefficients are defined in the following:

$$\begin{split} \mathcal{L}_{S}\hat{O} &\equiv \left[\hat{H}_{S},\hat{O}\right], \qquad \mathcal{Q}_{a}^{\times}\hat{O} \equiv \left[\hat{Q}_{a},\hat{O}\right], \qquad \mathcal{Q}_{a}^{\circ}\hat{O} \equiv \left\{\hat{Q}_{a},\hat{O}\right\}, \\ \eta'_{abk} &\equiv \frac{\eta_{abk} + \eta^{*}_{ab\overline{k}}}{2}, \qquad \eta''_{abk} \equiv \frac{\eta_{abk} - \eta^{*}_{ab\overline{k}}}{2i}. \end{split}$$

The RK-4/RK-45 algorithm<sup>69</sup> is usually adopted as the numerical propagation scheme of Eq. (23). There are also on-the-fly filtering algorithms available for acceleration.<sup>70</sup>

### D. Time-domain Prony fitting decomposition

In this context, the central problem in DEOM is to decompose the bare–bath TCF into a sum of exponential series. Based on FDT, this can be realized by expanding-over-pole strategies, such as Matsubara spectral decomposition (MSD)² and Padé spectral decomposition (PSD),  $^{71-73}$  or various least-square fitting schemes.  $^{74-77}$  The traditional expanding-over-poles strategies are usually restricted to certain forms of bath spectral density. Here, we choose the t-PFD strategy. The resulting numerical efficiency of HEOM/DEOM is optimized to a great extent, especially in low-temperature regimes that are usually inaccessible for other spectral decomposition methods, such as the MSD and PSD approaches.

The *t*-PFD scheme is intrinsically based on a least-squares fitting algorithm, in which the real and imaginary parts of TCF are fitted separately. It is easy to extract from the bosonic FDT [cf. Eq. (13)] that

$$\operatorname{Re}[C(t)] = \frac{1}{\pi} \int_{0}^{+\infty} d\omega \, J_{\text{eff}}(\omega; \beta) \coth\left(\frac{\beta\omega}{2}\right) \cos(\omega t)$$
$$= \frac{1}{\pi} \int_{0}^{+\infty} d\omega \, J(\omega) \cos(\omega t), \tag{24a}$$

$$\operatorname{Im}[C(t)] = -\frac{1}{\pi} \int_{0}^{+\infty} d\omega \, J_{\text{eff}}(\omega; \beta) \sin(\omega t)$$
$$= -\frac{1}{\pi} \int_{0}^{+\infty} d\omega \, J(\omega) \tanh(\beta \omega/2) \sin(\omega t), \qquad (24b)$$

where the second line in Eqs. (24a) and (24b) are the explicit results for S = 1/2 case. Intriguingly, temperature dependence is only carried by the imaginary part of TCF, in line with the fermion bath but the reverse of the boson bath.

Next, we target at optimizing  $K = K_r + K_i$  in

$$Re[C(t)] = \sum_{k=1}^{K_r} \zeta_k e^{-\lambda_k t}, \qquad Im[C(t)] = \sum_{k=1}^{K_i} \zeta'_k e^{-\lambda'_k t}, \qquad (25)$$

where  $K_r$  and  $K_i$  are the number of terms in real and imaginary part fitting, respectively. We accordingly denote the t-PFD strategy as  $K_r + K_i$ . See Ref. 64 and the reference therein for detailed procedures of t-PFD, as well as the numerical benchmarks for several commonly used spectral density functions. We also provide more illustrations and examples on the performances of TCF fitting using t-PFD in Appendix B, with respect to the most challenging SSB models we tested.

### E. Computational details

In this section, we present the numerical benchmark results of the bosonic DEOM equipped with *t*-PFD for various SSB models. The total Hamiltonian is in the following:

$$\hat{H}_{S} = \epsilon \hat{\sigma}_{z} + \Delta \hat{\sigma}_{x}, \tag{26a}$$

$$\hat{h}_{\rm B} = \sum_{i=1}^{N} \omega_j \hat{s}_z^j, \tag{26b}$$

$$\hat{H}_{SB} = \hat{\sigma}_z \otimes \sum_i \sqrt{2} c_j \hat{s}_x^j. \tag{26c}$$

We use the Ohmic form<sup>8</sup> with exponential cutoff for the description of the continuous bath and its interaction with the system,

$$J(\omega) = \frac{\pi}{2} \alpha \omega e^{-\omega/\omega_c}.$$
 (27)

In this expression,  $\alpha$  is the Kondo parameter that characterizes the system–bath coupling strength, and  $\omega_c$  is the bath cutoff frequency. Since Eq. (27) is defined via Eq. (4), it is proved to be in line with Eq. (9b), according to the discussions conducted in Sec. II B and Appendix A.

The DEOM propagation uses the fourth-order Runge–Kutta (RK-4) integrator with a time step of  $0.0025/\Delta$ , together with the on-the-fly filtering algorithm<sup>70</sup> with given error tolerance for acceleration.

### III. RESULTS AND DISCUSSIONS

### A. Zero-temperature spin relaxation dynamics and localization

Figure 1 shows the population dynamics  $P(t) \equiv \langle \hat{\sigma}_z(t) \rangle$  for zero-temperature unbiased SSB models (with  $\epsilon = 0$ , to keep in

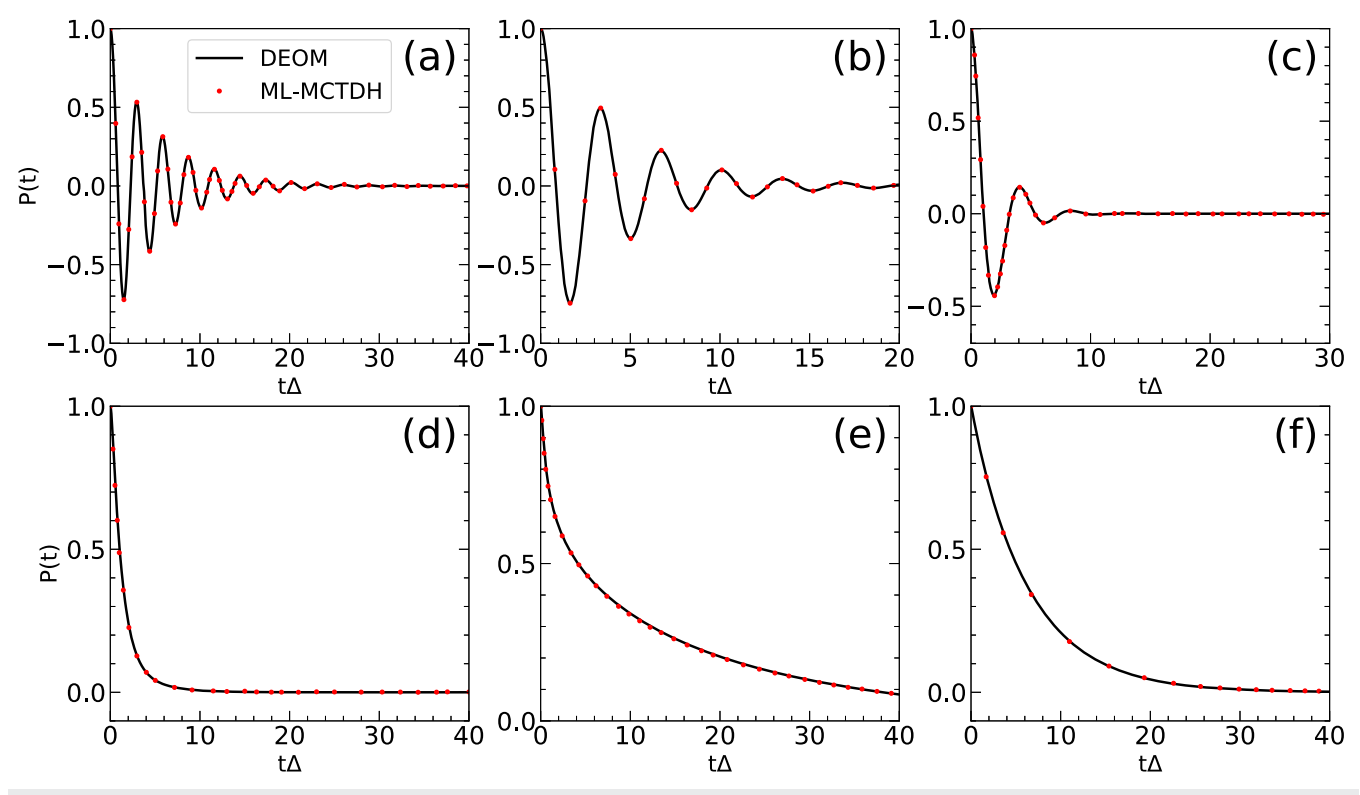


**FIG. 1.** Population dynamics of the zero-temperature SSB models. The spin baths are parameterized as (a)  $\alpha=0.5$  and  $\omega_c/\Delta=1$ . (b)  $\alpha=0.1$  and  $\omega_c/\Delta=6$ . (c)  $\alpha=0.2$  and  $\omega_c/\Delta=10$ . (d)  $\alpha=0.5$  and  $\omega_c/\Delta=10$ . (e)  $\alpha=0.75$  and  $\omega_c/\Delta=10$ . (f)  $\alpha=0.5$  and  $\omega_c/\Delta=10$ . The ML-MCTDH results are digitized from Ref. 33.

consistence with the previous work). Even though they are equal to the spin-boson models, they provide us with the first glimpse of the power of t-PFD. Here, we uniformly set the error tolerance of the on-the-fly filtering algorithm as  $5 \times 10^{-7}$ . We have also confirmed that the "empirical standard" error tolerance of  $1 \times 10^{-5}$  remains accurate enough in the present cases when  $\alpha \leq 0.5$ . For the model of Fig. 1(e) with coupling strength  $\alpha = 0.75$ , the convergence test suggests that the error tolerance should be set no larger than  $1 \times 10^{-6}$ All the numerically converged results are obtained with the *t*-PFD strategy 5 + 5 [Figs. 1(a)-1(d), and 1(f)] or 6 + 5 [Fig. 1(e)] to ensure the accuracy in TCF fitting and large enough number of tiers in the hierarchic expansion (here, 20 will be satisfying). The population dynamics obtained by DEOM (black solid lines) are compared to ML-MCTDH (red dots). In all the models presented, DEOM with t-PFD perfectly matches the ML-MCTDH results, including the Rabi oscillations and the incoherent relaxations.

Another important phenomenon about the unbiased SSB/spinboson model at zero temperature is *localization*, <sup>8</sup> which the population dynamics quickly reaches a biased stationary value. It is a typical phenomenon when the time scale of the bath is comparable with or longer than that of the subsystem. <sup>78–81</sup> Within the adiabatic or intermediate between the adiabatic and nonadiabatic regimes (that with a modest  $\omega_c/\Delta$  value), a large coupling strength ( $\alpha>1$ ) will bring about a large barrier height along the adiabatic double-well potential energy surface, such that localization of the population can be induced. <sup>33</sup>

Figure 2 shows the convergence test of the localization model (with  $\omega_c/\Delta=1, \alpha=10$ ) using different *t*-PFD strategies. This computation is rather challenging, as it generally requires a lot of memory and central processing unit (CPU) time to reach

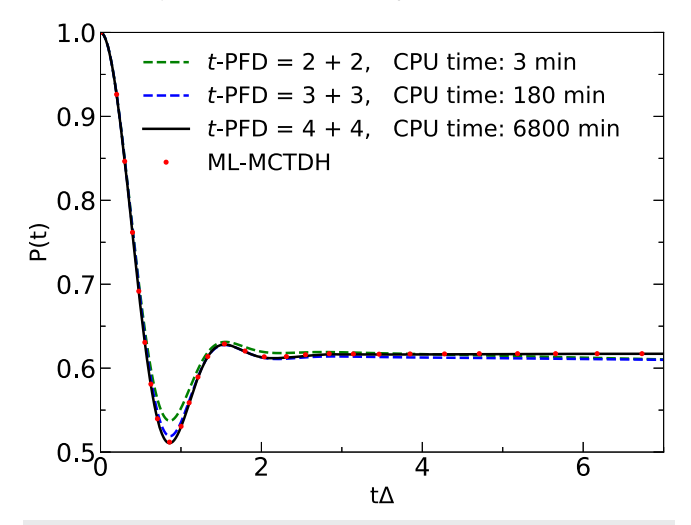


**FIG. 2.** Convergence test of the localization model ( $\omega_c/\Delta=1$ ,  $\alpha=10$ ) using t-PFD strategies 2 + 2, 3 + 3, and 4 + 4. Comparisons are made against ML-MCTDH (digitized from Ref. 33).

convergence. To ensure numerical accuracy and efficiency, we turn off the on-the-fly filtering module and set the number of tiers as 45 to stay accurate enough. The calculation is accelerated using the deom\_mpi package. Be a like of that the t-PFD strategy 2+2 is already able to capture the localization phenomenon, but is not accurate enough for population dynamics. At the expense of greater computational cost, the result generated with the t-PFD strategy 3+3 and 4+4 exhibits better accuracy. It takes more than 110 h of CPU time (Intel Xeon Gold 6330 CPU @2.00 GHz with 36 cores) with a memory requirement of no less than 300 GB to produce the 4+4 curve. The convergence is in good agreement with ML-MCTDH. See Appendix B also for details about the accuracy of TCF fitting under different t-PFD strategies.

## B. Finite-temperature spin relaxation dynamics and the localization-delocalization phase transition

Next, we turn to the finite-temperature cases. Figure 3 shows the temperature dependence of spin relaxation dynamics for several representative yet challenging SSB models.

In Fig. 3(a), P(t) under different temperatures, with bath parameters  $\omega_c/\Delta = 6$ ,  $\alpha = 0.5$  are shown [corresponding to Fig. 5(a) of Ref. 33]. All the curves are computed after reaching a good convergence using the t-PFD strategy 5 + 5. Figure 3(b) is similar to Fig. 3(a), but computationally more challenging, with  $\omega_c/\Delta = 10$ ,  $\alpha$  = 0.75 [corresponding to Fig. 6(c) of Ref. 33]. We take the *t*-PFD strategy 6 + 5 to reach the numerical convergence, even though 5 + 5will already be accurate enough. The comparisons are also made against ML-MCTDH. One can observe that at zero-temperature, the population dynamics clearly exhibits an incoherent decay to the equilibrium value P = 0. Increasing temperature by a little bit might greatly change the paradigm of decay; further increasing temperature will induce stronger coherent motion in a short time period. The temperature susceptibility is also closely related to the coupling strength  $\alpha$ .<sup>33</sup> It is well-known that at zero-temperature, the coherent-incoherent boundary is at  $\alpha = 0.5$  in the scaling limit.<sup>8</sup> For the SSB model, high temperature can significantly raise up this boundary value, as is also reported by Shao and Hänggi<sup>8</sup> as well as Forsythe and Makri.<sup>84</sup> It is very counter-intuitive yet interesting that higher temperature will slightly enhance the coherence for the central TLS in the nonadiabatic regime ( $\omega_c/\Delta \gg 1$ ). Physical interpretation of this abnormal phenomenon can be made from the analysis of the mapping spin-boson model with effective spectral density:  $J_{eff}(\omega)$  has a smaller magnitude when temperature increases, which renders weaker coupling to the central spin and win over the thermal excitation quenching effect, resulting in more coherent dynamics for the system TLS.33 Our results are in good agreement with the previous work.

Figure 3(c) shows the temperature-dependence of the localization model ( $\omega_c = 1, \alpha = 10$ ). All the curves are computed using the *t*-PFD strategy 4 + 4 with good convergence. As is observed when temperature increases, the population distribution gets a faster decay and the bias gradually disappears, which is actually a kind of *phase transition*.<sup>8,85</sup> This is because the increasing temperature will decrease the relaxation time of the bath so that the system TLS becomes *delocalized*.

Although our results show that DEOM with *t*-PFD are overall in excellent agreement with the ML-MCTDH results, we shall point out that for a certain number of finite-temperature models presented

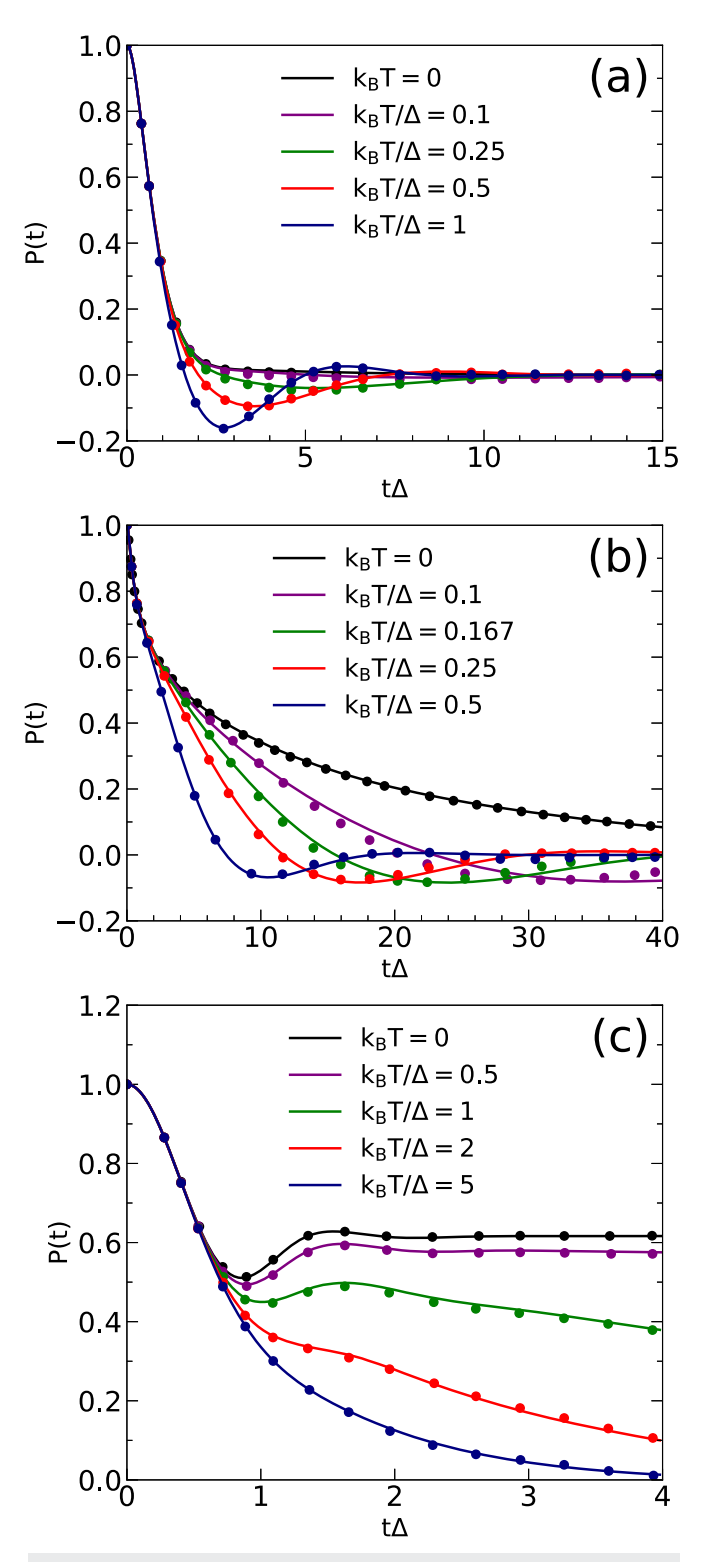


**FIG. 3.** Temperature-dependence in the coherent-incoherent transition of population dynamics. The spin bath models are parametrized as (a)  $\omega_c/\Delta=6$ ,  $\alpha=0.5$ . (b)  $\omega_c/\Delta=10$ ,  $\alpha=0.75$ . (c)  $\omega_c/\Delta=1$ ,  $\alpha=10$ . The DEOM results (solid lines) are compared to the ML-MCTDH results (solid dots, digitized from Ref. 33).

here, especially for the one with  $k_BT/\Delta=0.1$  and 0.167 shown in Fig. 3(b), there still exist minor discrepancies between DEOM and ML-MCTDH results even by eye inspection. This should be reasonable because ML-MCTDH adopts discretized bath modes and B–O type of approximation for high-frequency bath modes;<sup>33</sup> it is also susceptible to the tensor network propagation scheme, while HEOM/DEOM is able to use rigorously continuous bath modes. The major resource of error for HEOM/DEOM comes from the accuracy of bath TCF fitting after reaching convergence. Another possible reason lies in the finite-temperature strategy. ML-MCTDH adopts Monte Carlo importance sampling techniques<sup>86</sup> to evaluate the thermal Boltzmann operator, which is usually hard to reach numerical convergence, while HEOM/DEOM resorts to FDT being a *deterministic* pathway.

### C. More results on the finite-temperature biased models

As we know in realistic situations, the system is not always unbiased. For example, when a Zeeman field is applied to the central spin, the energy degeneracy will be broken, which is a common experimental setup to study the radical pair spin relaxation dynamics.<sup>24</sup> To this reason, we further study the spin relaxation dynamics for biased models under finite temperature and compare them to the corresponding spin-boson model with the same bath parameters.

Figure 4 shows the converged population dynamics and von Neumann entropy for several biased TLS (with  $\epsilon = \Delta$ ) interacting with a spin bath (SSB) or a boson bath (spin-boson). The von Neumann entropy reads as

$$S_{\rm vN}(t) \equiv -\operatorname{Tr}\left[\hat{\rho}_{\rm S}(t)\ln\,\hat{\rho}_{\rm S}(t)\right],\tag{28}$$

where  $\hat{\rho}_{S}(t)$  is the density matrix of the system TLS at time t. Three different models from high temperature ( $\beta = 0.25$ ) to low temperature ( $\beta = 5$ ) are presented here. As is observed for the high-temperature model shown in Fig. 4(a), the SSB model keeps

much better quantum coherence than the corresponding spin-boson model. The von Neumann entropy growth is also slower. As expected, when temperature decreases, the behavior of the SSB model gradually agrees with the spin-boson model. This can be understood straightforwardly from the temperature-dependent effective spectral density in Eq. (5) under different temperatures. As  $\beta \to \infty$ ,  $\tanh(\beta\omega/2) \to 1$  in a wider span of bath mode frequencies. It should be noted that the asymmetric TLS results presented here have not been reported previously.

### D. xy-xy type of couplings

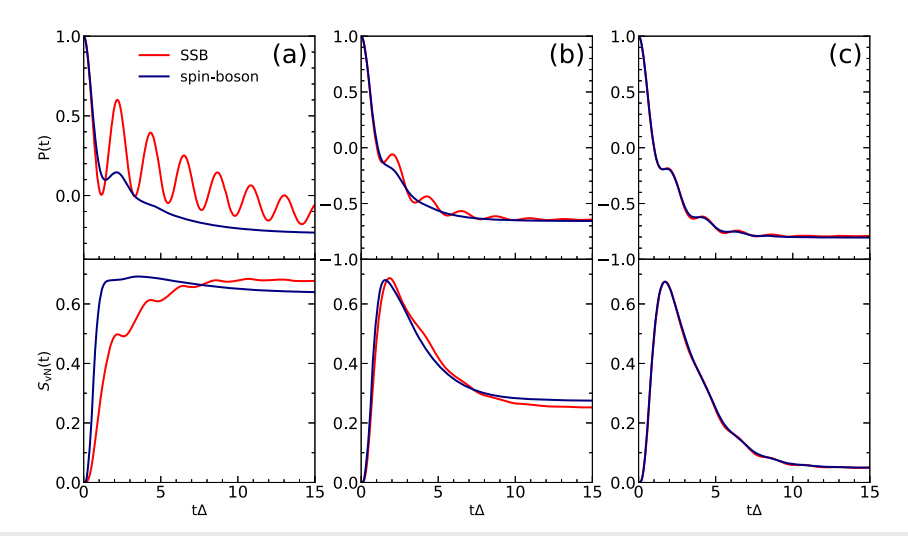
In this section, we provide numerical results for the more general SSB models, where the numerically exact DEOM results are compared to the approximated TCL-2 results. In particular, we focus on the xy-xy type of system-bath coupling, with

$$\hat{H}_{SB} = \frac{1}{\sqrt{S}} \sum_{j=1}^{N} c_j (\hat{s}_x^j \hat{\sigma}_x + \hat{s}_y^j \hat{\sigma}_y).$$
 (29)

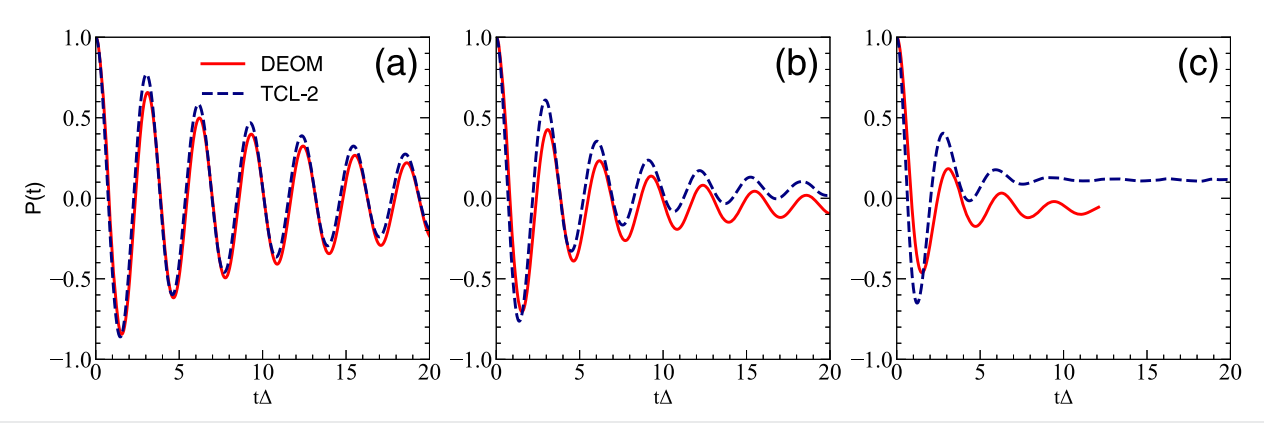
Under this case, the bath TCFs have cross terms [as shown in Eqs. (S42)–(S46) of the supplementary material], which are all temperature-dependent. Here, the system parameters are  $\epsilon=0$  and  $\Delta=1$ .

Figure 5 shows the population dynamics of the SSB model with xy–xy type of system–bath coupling, where we still assume an Ohmic spectral density for the spin bath. The DEOM results (red solid lines) are compared to the TCL-2 approach (dark blue dashed lines), with details provided in the supplementary material. One can see that in the short time regime, and for small  $\alpha$  cases, the TCL-2 results agree well with DEOM. While in the long-term regime, the TCL-2 results deviate from DEOM.

The above-mentioned examples have demonstrated the generality of the theoretical framework, as well as the accuracy and efficiency of the numerical implementations. In the supplementary material, we further provide numerical results for the z–x type of



**FIG. 4.** Population dynamics and von Neumann entropy of the biased SSB and spin-boson models. The boson/spin baths are parameterized as (a)  $\alpha=0.4$ ,  $\omega_c/\Delta=1$ , and  $\beta\Delta=0.25$ . (b)  $\alpha=0.4$ ,  $\omega_c/\Delta=2$ , and  $\beta\Delta=1.0$ . (c)  $\alpha=0.4$ ,  $\omega_c/\Delta=2$ , and  $\beta\Delta=5.0$ .



**FIG. 5.** Population dynamics of the SSB models with xy–xy type coupling, where the numerically exact DEOM results (red solid lines) are compared to the TCL-2 results (dark blue dashed lines). Here, we still assume an Ohmic spectral density for the spin environment with  $\omega_c = 1.0$ , and (a)  $\alpha = 0.1$ . (b)  $\alpha = 0.2$ . (c)  $\alpha = 0.4$ . The temperature is zero.

coupling  $\hat{H}_{SB} = \frac{1}{\sqrt{S}} \sum_{j=1}^{N} c_j \hat{s}_x^j \hat{\sigma}_z$ , as well as for the z–z type of coupling  $\hat{H}_{SB} = \frac{1}{\sqrt{S}} \sum_{j=1}^{N} c_j \hat{s}_z^j \hat{\sigma}_z$ . Models with xyz–xyz type of coupling can also be easily simulated based on the DEOM formalism and the spin-to-boson mapping relation.

#### IV. CONCLUDING REMARKS

We present the numerical benchmark results of the spin relaxation dynamics of various spin-spin-bath (SSB) models with continuous spectral density function by using DEOM with t-PFD. The idea of mapping boson bath with temperature-dependent effective spectral density is validated from a microscopic perspective and generalized to arbitrary bath spin quantum number S. The highlight of this strategy is that one can approximate a class of non-Gaussian bath to the Gaussian one under the linear response limit. By applying t-PFD to the bath TCF, one obtains the exponential decay basis to construct DEOM and propagate. The accuracy and numerical efficiency of this strategy are illustrated by various examples. DEOM with t-PFD provides an excellent agreement with the ML-MCTDH results reported in the literature, despite the rather challenging model parameters. Moreover, compared to a previous work on the SSB model based on ML-MCTDH, DEOM equipped with t-PFD has the advantage that the bath spectral density is rigorously continuous, and the finite-temperature strategy is based on FDT rather than stochastic sampling, thus allowing an efficient long-time propagation. In summary, the strategy demonstrated in the current work serves as a novel and more efficient benchmark scheme for quantum dynamics with a spin bath. In addition, we would like to comment on DEOM for spin 1/2 bath derived in Refs. 9 and 87, where the DEOM is derived based on a set of assumed dissipaton algebra, which includes certain mean-field approximations that have yet to be thoroughly examined. While it is equivalent to the current treatment in terms of the bare bath time-correlation function, there are some differences in the equations of motion. We anticipate that it may not necessarily yield results that are equivalent to those obtained with the current approach.

The presented theoretical work provides new insights into extending HEOM/DEOM to certain types of non-Gaussian

environments with arbitrary bath TCFs or spectral density functions. Future research work on methods development shall be carried out on more complicated types of interacting system-bath models that are listed in Eq. (3), with the incorporation of quadratic or higher order system-bath couplings, as well as the nonlinear response effects; we would also like to seek for applications in the simulation of radical pair spin relaxation dynamics that are exposed to an environment of nuclear spins.

#### SUPPLEMENTARY MATERIAL

See the <u>supplementary material</u> for additional information on the spin-to-boson mapping relation with a more general system-bath coupling and the numerical results for various types of SSB models, where the DEOM and second-order time-convolutionless (TCL-2) master equation are presented.

### **ACKNOWLEDGMENTS**

This work was supported by the National Science Foundation Award under Grant No. CHE-2244683. Computing resources were provided by the Center for Integrated Research Computing (CIRC) at the University of Rochester. W.Y. thanks YiJing Yan for his meticulous guidance when he was at USTC and for his valuable comments on this manuscript.

### **AUTHOR DECLARATIONS**

### **Conflict of Interest**

The authors have no conflicts to disclose.

#### **Author Contributions**

Wenxiang Ying: Conceptualization (lead); Data curation (lead); Formal analysis (lead); Investigation (lead); Methodology (lead); Software (lead); Validation (lead); Visualization (lead); Writing – original draft (lead); Writing – review & editing (lead). Yu Su:

Conceptualization (equal); Data curation (equal); Formal analysis (equal); Methodology (equal); Software (equal); Validation (equal); Writing – original draft (supporting); Writing – review & editing (equal). Zi-Hao Chen: Conceptualization (supporting); Formal analysis (supporting); Methodology (equal); Software (equal); Validation (equal); Writing – review & editing (supporting). Yao Wang: Conceptualization (equal); Formal analysis (equal); Methodology (equal); Project administration (equal); Software (equal); Supervision (equal); Validation (equal); Writing – review & editing (equal). Pengfei Huo: Conceptualization (equal); Formal analysis (supporting); Funding acquisition (lead); Investigation (supporting); Project administration (equal); Resources (equal); Supervision (equal); Writing – original draft (supporting); Writing – review & editing (equal).

### **DATA AVAILABILITY**

The data that support the findings of this work are available from the corresponding author under reasonable request.

### APPENDIX A: FDT FOR THE SPIN BATH AND THE EFFECTIVE BOSONIC ENVIRONMENT

### 1. S = 1/2 case

For spin-1/2 particles, we adopt the well-known Jordan–Wigner correspondence<sup>88</sup> for the spin operators,

$$\hat{d}_i^{\dagger} \equiv \hat{s}_x^j + i \hat{s}_y^j, \tag{A1a}$$

$$\hat{d}_j \equiv \hat{s}_x^j - i\hat{s}_y^j,\tag{A1b}$$

$$\hat{\mathbf{s}}_z^j = \hat{d}_j^\dagger \hat{d}_j - \frac{1}{2},\tag{A1c}$$

where  $\hat{d}_j$  and  $\hat{d}_j^{\dagger}$  are the mapping *fermionic* annihilation/creation operators with anti-commutation relation on the same site. On different sites, we have bosonic commutation relations, which mean spins on different sites commute, unlike fermions that are anti-commute. For this reason, spins are also referred to as *hard-core bosons* or *spinless fermions*, <sup>89</sup> whose commutation relations can be summarized as

$$\{\hat{d}_j, \hat{d}_j\} = \{\hat{d}_j^{\dagger}, \hat{d}_j^{\dagger}\} = 0, \qquad \{\hat{d}_j, \hat{d}_j^{\dagger}\} = 1,$$
 (A2a)

$$\{\hat{d}_j, \hat{d}_k\} = 2\hat{d}_j\hat{d}_k, \qquad \{\hat{d}_j^{\dagger}, \hat{d}_k^{\dagger}\} = 2\hat{d}_j^{\dagger}\hat{d}_k^{\dagger},$$

$$\{\hat{d}_j, \hat{d}_k^{\dagger}\} = 2\hat{d}_j \hat{d}_k^{\dagger}, \qquad k \neq j,$$
 (A2b)

$$\left[\hat{d}_{j},\hat{d}_{j}\right]=\left[\hat{d}_{j}^{\dagger},\hat{d}_{j}^{\dagger}\right]=0, \qquad \left[\hat{d}_{j},\hat{d}_{j}^{\dagger}\right]=1-2\hat{d}_{j}^{\dagger}\hat{d}_{j}, \qquad (A2c)$$

$$[\hat{d}_j, \hat{d}_k] = [\hat{d}_j^{\dagger}, \hat{d}_k^{\dagger}] = [\hat{d}_j, \hat{d}_k^{\dagger}] = 0, \quad k \neq j.$$
(A2d)

As is shown that the hard-core bosons possess characters of both bosons and fermions, one can either define the linear response functions using a commutator or the single-particle Green's function using an anti-commutator. Here, we will show both

possibilities. For convenience, let us first write down the time evolution of single bath operators,

$$\hat{d}_{j}^{\dagger}(t) = e^{i\hat{h}_{B}t} \hat{d}_{j}^{\dagger}(0) e^{-i\hat{h}_{B}t} = \hat{d}_{j}^{\dagger}(0) e^{i\omega_{j}t}, 
\hat{d}_{i}(t) = e^{i\hat{h}_{B}t} \hat{d}_{i}(0) e^{-i\hat{h}_{B}t} = \hat{d}_{i}(0) e^{-i\omega_{j}t},$$
(A3)

where we have used the well-known Baker–Campbell–Hausdorff identity. 90

We will start with the anti-commutator version. For each pair of mapping spinless fermionic creation/annihilation operators  $\hat{d}_{j}^{\dagger}$  and  $\hat{d}_{j}$  that satisfy the commutation relations defined in Eq. (A2), the single-particle Green's functions can be defined and evaluated as

$$\langle \{\hat{d}_{j}(t), \hat{d}_{k}^{\dagger}(0)\} \rangle_{B} = \delta_{jk}e^{-i\omega_{j}t},$$

$$\langle \{\hat{d}_{j}^{\dagger}(t), \hat{d}_{k}(0)\} \rangle_{B} = \delta_{jk}e^{i\omega_{j}t},$$

$$\langle \{\hat{d}_{j}(t), \hat{d}_{k}(0)\} \rangle_{B} = \langle \{\hat{d}_{j}^{\dagger}(t), \hat{d}_{k}^{\dagger}(0)\} \rangle_{B} = 0.$$
(A4)

So, we have

$$\langle \{\hat{F}(t), \hat{F}(0)\} \rangle_{\mathcal{B}} = \sum_{j} c_{j}^{2} \cos(\omega_{j} t). \tag{A5}$$

As a result, the spectral density function is evaluated as [cf. Eq.(9b)]

$$J'(\omega) = \frac{1}{2} \int_{-\infty}^{+\infty} dt \ e^{i\omega t} \langle \{\hat{F}(t), \hat{F}(0)\} \rangle_{B}$$
$$= \frac{\pi}{2} \sum_{i} c_{j}^{2} [\delta(\omega - \omega_{j}) + \delta(\omega + \omega_{j})], \tag{A6}$$

which is an extension of the result given by Caldeira and Leggett<sup>7</sup> [also see Eq. (4)] to negative frequencies  $\omega$  < 0, while ensuring it to be an even function.

The derivation via the commutator version is very similar to the anti-commutator one. Following the same procedure, one can easily obtain the bare-bath linear response function as

$$i\langle[\hat{F}(t),\hat{F}(0)]\rangle_{\rm B} = \sum_{i} c_{j}^{2}\langle(1-2\hat{d}_{j}^{\dagger}\hat{d}_{j})\rangle_{\rm B} \sin(\omega_{j}t).$$
 (A7)

For independent spin S = 1/2 particles, we have

$$Z_{\rm B} \equiv {\rm Tr}_{\rm B} \left[ e^{-\beta \hat{h}_{\rm B}} \right] = \prod_{j} 2 \cosh \left( \frac{\beta \omega_{j}}{2} \right),$$
 (A8)

one immediately obtains

$$i\langle [\hat{F}(t), \hat{F}(0)]\rangle_{B} = \sum_{j} c_{j}^{2} \tanh\left(\frac{\beta\omega_{j}}{2}\right) \sin(\omega_{j}t).$$
 (A9)

In addition, the corresponding spectral density function reads as [cf. Eq. (9a)]

$$J(\omega) = \frac{1}{2} \int_{-\infty}^{+\infty} dt \ e^{i\omega t} \langle [\hat{F}(t), \hat{F}(0)] \rangle_{B}$$
$$= \frac{\pi}{2} \sum_{i} c_{j}^{2} \tanh\left(\frac{\beta \omega_{j}}{2}\right) [\delta(\omega - \omega_{j}) - \delta(\omega + \omega_{j})], \quad (A10)$$

which is an odd function. On the other hand, we can rewrite Eq. (A10) as

$$J(\omega) = \frac{\pi}{2} \sum_{j} c_{j}^{2} \tanh\left(\frac{\beta\omega}{2}\right) \left[\delta(\omega - \omega_{j}) + \delta(\omega + \omega_{j})\right]$$
$$= J'(\omega) \tanh\left(\frac{\beta\omega}{2}\right), \tag{A11}$$

where  $J'(\omega)$  is defined in Eq. (A6), giving rise to the temperature-dependent effective spectral density.

Combining Eqs. (A5) and (A9), one obtains

$$\begin{split} C(t) &\equiv \langle \hat{F}(t)\hat{F}(0)\rangle_{\mathrm{B}} = \frac{1}{2}\sum_{j}c_{j}^{2}\left[\frac{e^{-i\omega_{j}t}}{1+e^{-\beta\omega_{j}}} + \frac{e^{i\omega_{j}t}}{1+e^{\beta\omega_{j}}}\right] \\ &= \frac{1}{2}\sum_{j}c_{j}^{2}\left[\delta(\omega-\omega_{j}) + \delta(\omega+\omega_{j})\right]\frac{e^{-i\omega t}}{1+e^{-\beta\omega}} \\ &= \frac{1}{\pi}\int_{-\infty}^{+\infty}d\omega\frac{e^{-i\omega t}J'(\omega)}{1+e^{-\beta\omega}}, \end{split} \tag{A12}$$

which is just Eq. (12) in the main text, the FDT for spin bath. It has an equivalent bosonic FDT formalism if one takes  $J_{\rm eff}(\omega;\beta)$   $\equiv J(\omega) = J'(\omega) \tanh(\beta \omega/2)$ , giving rise to Eq. (13). Thus, the spin-boson problem with an effective spectral density function arises naturally.

An alternative but similar argument can be made by using the coupled-fermion representation for spin operators (S = 1/2), discussed by Mattis *et al.*, <sup>39,91,92</sup> reading as

$$\hat{s}_{+}^{j} = \hat{c}_{i}^{\dagger} (\hat{d}_{j} + \hat{d}_{i}^{\dagger}), \tag{A13a}$$

$$\hat{s}_{-}^{j} = (\hat{d}_{i} + \hat{d}_{i}^{\dagger})\hat{c}_{i}, \tag{A13b}$$

$$\hat{\mathbf{s}}_z^j = \hat{c}_j^{\dagger} \hat{c}_j - \frac{1}{2},\tag{A13c}$$

where  $\hat{c}, \hat{c}^{\dagger}$  and  $\hat{d}, \hat{d}^{\dagger}$  are two sets of fermion operators that anti-commute with each other. On the other hand, since the mapping fermionic bath operators still commute with the system operators rather than anti-commute, it should also lead to the same bosonic DEOM formalism, as is studied by Jin *et al.* 93 based on the influence functional.

### 2. Generalization to arbitrary spin S

Adopting the same angular momentum raising/lowering operators that are defined as

$$\hat{s}_{+}^{j} \equiv \hat{s}_{x}^{j} + i\hat{s}_{y}^{j}, \qquad \hat{s}_{-}^{j} \equiv \hat{s}_{x}^{j} - i\hat{s}_{y}^{j},$$
 (A14)

so that the original  $\bigotimes_{i=1}^{N} \mathfrak{su}(2)$  Lie algebra becomes

$$[\hat{s}_{+}^{i}, \hat{s}_{-}^{j}] = 2\hat{s}_{z}^{i}\delta_{ij}, \qquad [\hat{s}_{z}^{i}, \hat{s}_{+}^{j}] = \pm \hat{s}_{\pm}^{i}\delta_{ij}.$$
 (A15)

Their time dependence can be evaluated as

$$\hat{s}_{\pm}^{j}(t) = e^{i\hat{h}_{B}t} \hat{s}_{\pm}^{j}(0) e^{-i\hat{h}_{B}t} = \hat{s}_{\pm}^{j}(0) e^{\pm i\omega_{j}t}. \tag{A16}$$

The bare-bath partition function can be evaluated as

$$Z_{\rm B} = \prod_{j} \left( 2\sum_{k=0}^{[S]} \cosh\left( (k + \{S\})\beta\omega_{j} \right) - \Delta(S) \right), \tag{A17}$$

where [S] and  $\{S\}$  are the integer and fractional part of S, respectively, with  $S = [S] + \{S\}$ ;  $\Delta(S) = 1$  for S being integers; and  $\Delta(S) = 0$  for S being half integers. As a result,

$$\langle \hat{\mathbf{s}}_{z}^{j} \rangle_{\mathrm{B}} = -\frac{\partial \ln Z_{\mathrm{B}}}{\partial (\beta \omega_{j})}, \qquad \langle (\hat{\mathbf{s}}_{z}^{j})^{2} \rangle_{\mathrm{B}} = \frac{\partial^{2} \ln Z_{\mathrm{B}}}{\partial (\beta \omega_{j})^{2}}.$$
 (A18)

It is also easy to obtain the bare-bath single particle Green's function and linear response function as

$$\langle \{\hat{F}(t), \hat{F}(0)\} \rangle_{B} = \frac{1}{S} \sum_{j} c_{j}^{2} [S(S+1) - \langle (\hat{s}_{z}^{j})^{2} \rangle_{B}] \cos(\omega_{j}t), \quad (A19a)$$

$$i\langle [\hat{F}(t), \hat{F}(0)] \rangle_{B} = -\frac{1}{S} \sum_{j} c_{j}^{2} \langle \hat{s}_{z}^{j} \rangle_{B} \sin(\omega_{j}t).$$
 (A19b)

In addition, the corresponding spectral density functions can be evaluated by Eqs. (9a) and (9b) as

$$J'(\omega) = \frac{\pi}{2S} \sum_{j} c_{j}^{2} [S(S+1) - \langle (\hat{s}_{z}^{j})^{2} \rangle_{B}] [\delta(\omega - \omega_{j}) + \delta(\omega + \omega_{j})],$$
(A20a)

$$J(\omega) = -\frac{\pi}{2S} \sum_{i} c_{j}^{2} \langle \hat{s}_{z}^{j} \rangle_{B} [\delta(\omega - \omega_{j}) - \delta(\omega + \omega_{j})]. \tag{A20b}$$

They are derived from a microscopic perspective, satisfying the correct symmetry; however, neither of them gives rise to the original definition of bath spectral density function given by Caldeira and Leggett. One might choose to still use Eq. (4) and directly get  $J(\omega)$  in Eq. (A20b) as the effective spectral density or perform modifications to make it in accordance with Eq. (A20a) or (A20b). For example, if we use [cf. Eq. (A20a)]

$$J'(\omega) = \frac{\pi}{2S} \sum_{j} c_{j}^{2} \left[ S(S+1) - \langle (\hat{s}_{z}^{j})^{2} \rangle_{B} \right]_{\omega_{j} = \omega} \left[ \delta(\omega - \omega_{j}) + \delta(\omega + \omega_{j}) \right], \tag{A21}$$

where the footnote  $\omega_j = \omega$  means replacing all the  $\omega_j$  in the prefactors by  $\omega$ . Then, the theory of effective spectral density function can arise as

$$C(t) = \langle \hat{F}(t)\hat{F}(0)\rangle_{B} = \frac{1}{\pi} \int_{-\infty}^{+\infty} d\omega e^{-i\omega t} \frac{J_{\text{eff}}(\omega; \beta, S)}{1 - e^{-\beta\omega}},$$

$$J_{\text{eff}}(\omega; \beta, S) = J(\omega) = J'(\omega)\zeta(\omega; \beta, S),$$
(A22)

with

$$\zeta(\omega;\beta,S) \equiv \frac{1 - e^{-\beta\omega}}{2} \times \frac{S(S+1) - \langle (\hat{s}_z^j)^2 \rangle_{B} - \langle \hat{s}_z^j \rangle_{B}}{S(S+1) - \langle (\hat{s}_z^j)^2 \rangle_{B}} \bigg|_{\omega_i = \omega}. \quad (A23)$$

One can check that  $\zeta(\omega; \beta, S = 1/2) = \tanh(\beta \omega/2)$ .

On the other hand, under the high spin limit of  $S \gg 1$ , Eq. (A20b) will reduce to the conventional form,

$$J(\omega) = \frac{\pi}{2} \sum_{j} c_{j}^{2} [\delta(\omega - \omega_{j}) - \delta(\omega + \omega_{j})], \qquad (A24)$$

which is in line with the original definition in Eq. (4) but with odd analytical continuation. As a result, the spin bath under the high spin limit is isomorphic to the boson bath. This can be understood via the Holstein–Primakoff transformation, <sup>94</sup>

$$\hat{s}_{+}^{i} = \sqrt{2S} \sqrt{1 - \frac{\hat{b}_{i}^{\dagger} \hat{b}_{i}}{2S}} \hat{b}_{i} \approx \sqrt{2S} \hat{b}_{i},$$

$$\hat{s}_{-}^{i} = \sqrt{2S} \hat{b}_{i}^{\dagger} \sqrt{1 - \frac{\hat{b}_{i}^{\dagger} \hat{b}_{i}}{2S}} \approx \sqrt{2S} \hat{b}_{i}^{\dagger},$$

$$\hat{s}_{z}^{i} = S - \hat{b}_{i}^{\dagger} \hat{b}_{i},$$
(A25)

where  $\hat{b}_i^{\dagger}$  and  $\hat{b}_i$  are bosonic creation/annihilation operators that satisfy the Heisenberg commutation relations. Consequently,

$$\hat{F} = \frac{1}{\sqrt{S}} \sum_{j} c_j \hat{s}_x^j \approx \sum_{j} \frac{c_j}{\sqrt{2}} (\hat{b}_j + \hat{b}_j^{\dagger}) \equiv \sum_{j} c_j \hat{x}_j, \tag{A26}$$

where  $\hat{x}_j \equiv (\hat{b}_j + \hat{b}_j^{\dagger})/\sqrt{2}$ . Equation (A26) recovers the bath dissipation operator of the conventional spin-boson model.

One should find it straightforward to generalize the discussions above to more complicated interacting system–bath models, which might contain multiple dissipation modes, as listed in Eq. (3), by carrying out very similar arguments. The spectral density functions will be anisotropic in such cases. Even more general, the linear response limit can be easily applied to general finite baths,  $^{28,95}$  with multiple dissipation modes, *i.e.*, the individual bath particles are general level systems with SU(N) symmetry. In these situations, the generators of  $\mathfrak{su}(N)$  Lie algebra  $^{96,97}$  can be applied. Another pathway to establish the theory of effective spectral density function could be achieved by using the generalized Schwinger's theory of angular momentum,  $^{98}$  which remains to be further explored.

### APPENDIX B: THE NUMERICAL ACCURACY OF t-PFD STRATEGIES

In this section, we will provide examples of different *t*-PFD strategies to illustrate their numerical accuracy on TCF fitting.

Figure 6 shows the *t*-PFD results for the real and imaginary parts of bare-bath TCFs. We take the most challenging model with bath parameters  $\omega_c/\Delta=1$ ,  $\alpha=10$ , and the bare-bath TCF plateau time is taken as  $40\Delta$  with resolution  $dt=0.01\Delta$  uniformly. Figures 6(a) and 6(b) show the accuracy of fitting for the zero-temperature model using different numbers of terms. Figures 6(a) and 6(b) show the accurate enough to fit the real and imaginary parts of the TCF, respectively. Figures 6(c) and 6(d) show the fitting results of finite-temperature models using the 4 + 4 scheme. It is observed straightforwardly that the real part of TCF is

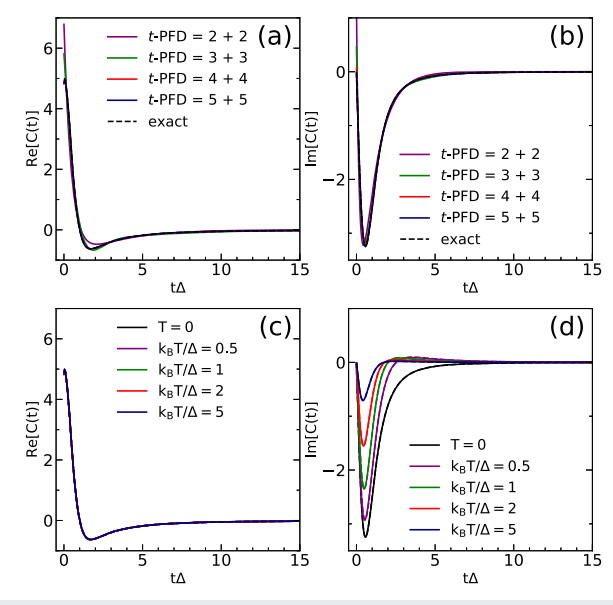


**FIG. 6.** *t*-PFD fitting results for the spin bath with  $\omega_c/\Delta=1$ ,  $\alpha=10$ . Panels (a) and (b): real and imaginary part fitting results for the zero-temperature model using 2, 3, 4, and 5 terms, respectively. Panels (c) and (d): real and imaginary part fitting results for different finite-temperature models using four terms; the dashed lines represent the exact TCF, and the solid lines represent the fitting results, which are almost overlapped.

temperature-independent, and only the imaginary part varies with temperature, in accordance with Eq. (24). The finite-temperature models are expected to be more difficult to be accurately fitted than the zero-temperature model. Here, all curves are accurately fitted using the 4 + 4 scheme by eye inspection.

In summary, to reach better accuracy, one will need to use more terms, but the expense is that the computational cost grows drastically. For practical use, one will need to explore the proper t-PFD strategy to balance accuracy and computational cost with regard to the specific bath types and parameters.

### REFERENCES

<sup>1</sup>A. J. Leggett, S. Chakravarty, A. T. Dorsey, M. P. A. Fisher, A. Garg, and W. Zwerger, "Dynamics of the dissipative two-state system," Rev. Mod. Phys. **59**, 1–85 (1987).

<sup>2</sup>U. Weiss, Quantum Dissipation Systems (World Scientific, Singapore, 1993).

<sup>3</sup> A. Nitzan, Chemical Dynamics in Condensed Phases (Oxford University Press, 2006)

<sup>4</sup>P. Hänggi, P. Talkner, and M. Borkovec, "Reaction-rate theory: Fifty years after kramers," Rev. Mod. Phys. **62**, 251–341 (1990).

<sup>5</sup> A. G. Kofman and G. Kurizki, "Unified theory of dynamically suppressed qubit decoherence in thermal baths," Phys. Rev. Lett. 93, 130406 (2004).

<sup>6</sup>S. Hammes-Schiffer and A. A. Stuchebrukhov, "Theory of coupled electron and proton transfer reactions," Chem. Rev. 110, 6939–6960 (2010).

<sup>7</sup> A. Caldeira and A. Leggett, "Quantum tunnelling in a dissipative system," Ann. Phys. 149, 374–456 (1983).

<sup>8</sup> A. O. Caldeira, A. H. Castro Neto, and T. Oliveira de Carvalho, "Dissipative quantum systems modeled by a two-level-reservoir coupling," Phys. Rev. B 48, 13974–13976 (1993).

- <sup>9</sup>Y. J. Yan, "Theory of open quantum systems with bath of electrons and phonons and spins: Many-dissipaton density matrixes approach," J. Chem. Phys. **140**, 054105 (2014).
- <sup>10</sup> N. V. Prokof ev and P. C. E. Stamp, "Low-temperature quantum relaxation in a system of magnetic nanomolecules," Phys. Rev. Lett. **80**, 5794–5797 (1998).
- <sup>11</sup>W. Wernsdorfer, T. Ohm, C. Sangregorio, R. Sessoli, D. Mailly, and C. Paulsen, "Observation of the distribution of molecular spin states by resonant quantum tunneling of the magnetization," Phys. Rev. Lett. **82**, 3903–3906 (1999).
- 12 W. Wernsdorfer, R. Sessoli, and D. Gatteschi, "Nuclear-spin-driven resonant tunnelling of magnetisation in Mn<sub>12</sub> acetate," Europhys. Lett. 47, 254–259 (1999).
   13 W. Wernsdorfer, A. Caneschi, R. Sessoli, D. Gatteschi, A. Cornia, V. Villar, and C. Paulsen, "Effects of nuclear spins on the quantum relaxation of the magnetization for the molecular nanomagnet Fe<sub>8</sub>," Phys. Rev. Lett. 84, 2965–2968 (2000).
- <sup>14</sup>N. A. Sinitsyn and N. Prokof'ev, "Nuclear spin bath effects on Landau-Zener transitions in nanomagnets," Phys. Rev. B 67, 134403 (2003).
- <sup>15</sup> A. Steane, "Quantum computing," Rep. Prog. Phys. **61**, 117–173 (1998).
- <sup>16</sup>M. V. G. Dutt, J. Cheng, B. Li, X. Xu, X. Li, P. R. Berman, D. G. Steel, A. S. Bracker, D. Gammon, S. E. Economou, R.-B. Liu, and L. J. Sham, "Stimulated and spontaneous optical generation of electron spin coherence in charged gaas quantum dots," Phys. Rev. Lett. 94, 227403 (2005).
- <sup>17</sup>H. M. Rønnow, R. Parthasarathy, J. Jensen, G. Aeppli, T. F. Rosenbaum, and D. F. McMorrow, "Quantum phase transition of a magnet in a spin bath," Science **308**, 389–392 (2005).
- <sup>18</sup>J. Du, X. Rong, N. Zhao, Y. Wang, J. Yang, and R. B. Liu, "Preserving electron spin coherence in solids by optimal dynamical decoupling," Nature 461, 1265–1268 (2009).
- <sup>19</sup>N. Zhao, S.-W. Ho, and R.-B. Liu, "Decoherence and dynamical decoupling control of nitrogen vacancy center electron spins in nuclear spin baths," Phys. Rev. B **85**, 115303 (2012).
- <sup>20</sup> W. H. Zurek, "Decoherence and the transition from quantum to classical," Phys. Today 44(10), 36 (1991).
- <sup>21</sup> J. R. Anglin, J. P. Paz, and W. H. Zurek, "Deconstructing decoherence," Phys. Rev. A 55, 4041–4053 (1997).
- <sup>22</sup>G. A. Álvarez, D. Suter, and R. Kaiser, "Localization-delocalization transition in the dynamics of dipolar-coupled nuclear spins," Science 349, 846–848 (2015).
- A. Gómez-León and P. C. E. Stamp, "Dynamical quantum phase transitions in presence of a spin bath," Phys. Rev. B 95, 054402 (2017).
   T. P. Fay, L. P. Lindoy, and D. E. Manolopoulos, "Electron spin relaxation in
- T. P. Fay, L. P. Lindoy, and D. E. Manolopoulos, "Electron spin relaxation in radical pairs: Beyond the redfield approximation," J. Chem. Phys. **151**, 154117 (2019).
- <sup>25</sup>T. P. Fay, L. P. Lindoy, D. E. Manolopoulos, and P. J. Hore, "How quantum is radical pair magnetoreception?," Faraday Discuss. 221, 77–91 (2020).
- <sup>26</sup>S. M. Harvey and M. R. Wasielewski, "Photogenerated spin-correlated radical pairs: From photosynthetic energy transduction to quantum information science," J. Am. Chem. Soc. 143, 15508–15529 (2021).
- <sup>27</sup> S. L. Bayliss, D. W. Laorenza, P. J. Mintun, B. D. Kovos, D. E. Freedman, and D. D. Awschalom, "Optically addressable molecular spins for quantum information processing," Science 370, 1309–1312 (2020).
- <sup>28</sup> A. Suárez and R. Silbey, "Properties of a macroscopic system as a thermal bath," J. Chem. Phys. **95**, 9115–9121 (1991).
- <sup>29</sup>N. Makri, "Iterative evaluation of the path integral for a system coupled to an anharmonic bath," J. Chem. Phys. **111**, 6164–6167 (1999).
- <sup>30</sup>Y.-A. Yan, "Stochastic simulation of anharmonic dissipation. I. Linear response regime," J. Chem. Phys. **145**, 204111 (2016).
- <sup>31</sup>N. Makri, "The linear response approximation and its lowest order corrections: An influence functional approach," J. Phys. Chem. B 103, 2823–2829 (1999).
- <sup>32</sup>N. Makri, "Small matrix modular path integral: Iterative quantum dynamics in space and time," Phys. Chem. Chem. Phys. **23**, 12537–12540 (2021).
- H. Wang and J. Shao, "Dynamics of a two-level system coupled to a bath of spins," J. Chem. Phys. 137, 22A504 (2012).
   D. Gelman, C. P. Koch, and R. Kosloff, "Dissipative quantum dynamics with
- <sup>54</sup>D. Gelman, C. P. Koch, and R. Kosloff, "Dissipative quantum dynamics with the surrogate Hamiltonian approach. A comparison between spin and harmonic baths," J. Chem. Phys. **121**, 661–671 (2004).

- <sup>35</sup>F. Habecker, R. Röhse, and T. Klüner, "Dissipative quantum dynamics using the stochastic surrogate Hamiltonian approach," J. Chem. Phys. **151**, 134113 (2019).
- <sup>36</sup>N. Wu and Y. Zhao, "Dynamics of a two-level system under the simultaneous influence of a spin bath and a boson bath," J. Chem. Phys. **139**, 054118 (2013).
- <sup>37</sup>E. Barnes, L. Cywiński, and S. Das Sarma, "Master equation approach to the central spin decoherence problem: Uniform coupling model and role of projection operators," Phys. Rev. B **84**, 155315 (2011).
- <sup>38</sup>C.-Y. Hsieh and J. Cao, "A unified stochastic formulation of dissipative quantum dynamics. I. Generalized hierarchical equations," J. Chem. Phys. **148**, 014103 (2018).
- <sup>39</sup>C.-Y. Hsieh and J. Cao, "A unified stochastic formulation of dissipative quantum dynamics. II. Beyond linear response of spin baths," J. Chem. Phys. 148, 014104 (2018).
- <sup>40</sup>Z. Lü and H. Zheng, "Influence of temperature on coherent dynamics of a two-level system immersed in a dissipative spin bath," J. Chem. Phys. 131, 134503 (2009).
- <sup>41</sup>A. A. Golosov, S. I. Tsonchev, P. Pechukas, and R. A. Friesner, "Spin-spin model for two-level system/bath problems: A numerical study," J. Chem. Phys. 111, 9918–9923 (1999).
- <sup>42</sup>W. M. Witzel and S. Das Sarma, "Concatenated dynamical decoupling in a solid-state spin bath," Phys. Rev. B **76**, 241303 (2007).
- <sup>43</sup>W. Yao, R.-B. Liu, and L. J. Sham, "Theory of electron spin decoherence by interacting nuclear spins in a quantum dot," Phys. Rev. B **74**, 195301 (2006).
- <sup>44</sup>W. Yang and R.-B. Liu, "Quantum many-body theory of qubit decoherence in a finite-size spin bath," Phys. Rev. B **78**, 085315 (2008).
- <sup>45</sup>Z.-S. Yang, Y.-X. Wang, M.-J. Tao, W. Yang, M. Zhang, Q. Ai, and F.-G. Deng, "Longitudinal relaxation of a nitrogen-vacancy center in a spin bath by generalized cluster-correlation expansion method," Ann. Phys. **413**, 168063 (2020).
- <sup>46</sup>S. K. Saikin, W. Yao, and L. J. Sham, "Single-electron spin decoherence by nuclear spin bath: Linked-cluster expansion approach," Phys. Rev. B **75**, 125314 (2007).
- <sup>47</sup>T. Gräßer, P. Bleicker, D.-B. Hering, M. Yarmohammadi, and G. S. Uhrig, "Dynamic mean-field theory for dense spin systems at infinite temperature," Phys. Rev. Res. 3, 043168 (2021).
- <sup>48</sup>K. Nakamura and Y. Tanimura, "Open quantum dynamics theory for a complex subenvironment system with a quantum thermostat: Application to a spin heat bath," J. Chem. Phys. **155**, 244109 (2021).
- <sup>49</sup>H. Kleinert, Path Integrals in Quantum Mechanics, Statistics, Polymer Physics, and Financial Markets, 5th ed. (World Scientific, Singapore, 2009).
- <sup>50</sup>L. P. Lindoy and D. E. Manolopoulos, "Simple and accurate method for central spin problems," Phys. Rev. Lett. **120**, 220604 (2018).
- <sup>51</sup> T. P. Fay, L. P. Lindoy, and D. E. Manolopoulos, "Spin-selective electron transfer reactions of radical pairs: Beyond the Haberkorn master equation," J. Chem. Phys. **149**, 064107 (2018).
- <sup>52</sup>L. P. Lindoy, T. P. Fay, and D. E. Manolopoulos, "Quantum mechanical spin dynamics of a molecular magnetoreceptor," J. Chem. Phys. 152, 164107 (2020).
- <sup>53</sup>T. P. Fay, L. P. Lindoy, and D. E. Manolopoulos, "Spin relaxation in radical pairs from the stochastic Schrödinger equation," J. Chem. Phys. 154, 084121 (2021).
- <sup>54</sup>N. Makri, "Small matrix path integral for system-bath dynamics," J. Chem. Theory Comput. **16**, 4038–4049 (2020).
- <sup>55</sup>N. Makri, "Small matrix decomposition of Feynman path amplitudes," J. Chem. Theory Comput. 17, 3825–3829 (2021).
- <sup>56</sup>D. E. Makarov and N. Makri, "Path integrals for dissipative systems by tensor multiplication. Condensed phase quantum dynamics for arbitrarily long time," Chem. Phys. Lett. 221, 482–491 (1994).
- <sup>57</sup>N. Makri, "Numerical path integral techniques for long time dynamics of quantum dissipative systems," J. Math. Phys. 36, 2430–2457 (1995).
- <sup>58</sup> D. Segal, A. J. Millis, and D. R. Reichman, "Numerically exact path-integral simulation of nonequilibrium quantum transport and dissipation," Phys. Rev. B **82**, 205323 (2010).
- <sup>59</sup>H. D. Meyer, F. Gatti, and G. A. Worth, Multidimensional Quantum Dynamics: MCTDH Theory and Applications (Wiley-VCH Verlag GmbH & Co. KGaA, 2009)
- <sup>60</sup>Y. Tanimura, "Nonperturbative expansion method for a quantum system coupled to a harmonic-oscillator bath," Phys. Rev. A **41**, 6676–6687 (1990).

- 61 Y. Tanimura, "Stochastic Liouville, Langevin, Fokker-Planck, and master equation approaches to quantum dissipative systems," J. Phys. Soc. Jpn. 75, 082001
- 62 R.-X. Xu, P. Cui, X.-Q. Li, Y. Mo, and Y. Yan, "Exact quantum master equation via the calculus on path integrals," J. Chem. Phys. 122, 041103 (2005).
- 63 Y. Yan, J. Jin, R.-X. Xu, and X. Zheng, "Dissipation equation of motion approach to open quantum systems," Front. Phys. 11, 110306 (2016).
- <sup>64</sup>Z.-H. Chen, Y. Wang, X. Zheng, R.-X. Xu, and Y. Yan, "Universal timedomain prony fitting decomposition for optimized hierarchical quantum master equations," J. Chem. Phys. 156, 221102 (2022).
- <sup>65</sup>E. Ising, "Beitrag zur theorie des ferromagnetismus," Z. Phys. 31, 253–258 (1925).
- <sup>66</sup>P. A. M. Dirac, "Quantum mechanics of many-electron systems," Proc. R. Soc. London, Ser. A 123, 714-733 (1929).
- 67D. D. Bhaktavatsala Rao and G. Kurizki, "From zeno to anti-zeno regime: Decoherence-control dependence on the quantum statistics of the bath," Phys. Rev. A 83, 032105 (2011).
- <sup>68</sup> Note that historically, Schotte<sup>100</sup> first pointed out that at low temperature and long time limit  $(t \gg \omega_s^{-1})$ , the dynamics given by the Kondo Hamiltonian in a bosonic picture is the same as that of the corresponding fermionic operators. This pattern also emerges in the theoretical validation of the Caldeira-Leggett model. <sup>7,8</sup> <sup>69</sup>R. L. Burden and J. D. Faires, *Numerical Analysis*, 9th ed. (Brooks/Cole, Cengage
- Learning, 2011).
- <sup>70</sup>Q. Shi, L. Chen, G. Nan, R.-X. Xu, and Y. Yan, "Efficient hierarchical Liouville space propagator to quantum dissipative dynamics," J. Chem. Phys. 130, 084105
- <sup>71</sup>T. Ozaki, "Continued fraction representation of the Fermi-Dirac function for large-scale electronic structure calculations," Phys. Rev. B 75, 035123 (2007).
- 72 J. Hu, R.-X. Xu, and Y. Yan, "Communication: Padé spectrum decomposition of Fermi function and Bose function," J. Chem. Phys. 133, 101106 (2010).
- <sup>73</sup> J. Hu, M. Luo, F. Jiang, R.-X. Xu, and Y. Yan, "Padé spectrum decompositions of quantum distribution functions and optimal hierarchical equations of motion construction for quantum open systems," J. Chem. Phys. 134, 244106 (2011).
- <sup>74</sup>H. Liu, L. Zhu, S. Bai, and Q. Shi, "Reduced quantum dynamics with arbitrary bath spectral densities: Hierarchical equations of motion based on several different bath decomposition schemes," J. Chem. Phys. 140, 134106 (2014).
- 75 C. Duan, Q. Wang, Z. Tang, and J. Wu, "The study of an extended hierarchy equation of motion in the spin-boson model: The cutoff function of the sub-ohmic spectral density," J. Chem. Phys. 147, 164112 (2017).
- <sup>76</sup>Q. Wang, Z. Gong, C. Duan, Z. Tang, and J. Wu, "Dynamical scaling in the ohmic spin-boson model studied by extended hierarchical equations of motion," J. Chem. Phys. 150, 084114 (2019).
- 77N. Lambert, S. Ahmed, M. Cirio, and F. Nori, "Modelling the ultra-strongly coupled spin-boson model with unphysical modes," Nat. Commun. 10, 3721
- <sup>78</sup>F. B. Anders, R. Bulla, and M. Vojta, "Equilibrium and nonequilibrium dynamics of the sub-ohmic spin-boson model," Phys. Rev. Lett. 98, 210402 (2007).
- <sup>79</sup>H. Wang and M. Thoss, "From coherent motion to localization: Dynamics of the spin-boson model at zero temperature," New J. Phys. 10, 115005 (2008).
- <sup>80</sup>H. Wang and M. Thoss, "From coherent motion to localization: II. Dynamics of the spin-boson model with sub-ohmic spectral density at zero temperature," Chem. Phys. 370, 78-86 (2010), dynamics of molecular systems: From quantum
- <sup>81</sup>C. Duan, Z. Tang, J. Cao, and J. Wu, "Zero-temperature localization in a sub-ohmic spin-boson model investigated by an extended hierarchy equation of motion," Phys. Rev. B 95, 214308 (2017).

- 82 See https://github.com/chem12346789/deom mpi for more information about the DEOM codes with CPU parallelization.
- 83 J. Shao and P. Hänggi, "Decoherent dynamics of a two-level system coupled to a sea of spins," Phys. Rev. Lett. 81, 5710-5713 (1998).
- <sup>84</sup>K. M. Forsythe and N. Makri, "Dissipative tunneling in a bath of two-level systems," Phys. Rev. B 60, 972-978 (1999).
- ${}^{\bf 85}\text{E.}$  Y. Wilner, H. Wang, M. Thoss, and E. Rabani, "Sub-ohmic to super-ohmic crossover behavior in nonequilibrium quantum systems with electron-phonon interactions," Phys. Rev. B 92, 195143 (2015).
- <sup>86</sup>H. Wang and M. Thoss, "Quantum-mechanical evaluation of the Boltzmann operator in correlation functions for large molecular systems: A multilayer multiconfiguration time-dependent Hartree approach," J. Chem. Phys. 124, 034114
- 87 H. D. Zhang, R.-X. Xu, X. Zheng, and Y. Yan, "Nonperturbative spin-boson and spin-spin dynamics and nonlinear Fano interferences: A unified dissipaton theory based study," J. Chem. Phys. 142, 024112 (2015).
- <sup>88</sup>P. Jordan and E. Wigner, "Über das paulische Äquivalenzverbot," Z. Phys. 47, 631-651 (1928).
- $^{\bf 89}{\rm M.}$  Girardeau, "Relationship between systems of impenetrable bosons and fermions in one dimension," J. Math. Phys. 1, 516-523 (1960).
- 90 B. C. Hall, GTM222: Lie Groups, Lie Algebras, and Representations, an Elementary Introduction, 2nd ed. (Springer, Switzerland, 2015).
- <sup>91</sup>D. C. Mattis, The Theory of Magnetism (Springer, 1965).
- 92 Y. Wang, S. Shtrikman, and H. Callen, "Wick's theorem for spin operators and its relation to the coupled-fermion representation," J. Appl. Phys. 37, 1451-1452 (1966).
- 93 J. Jin, S. Welack, J. Luo, X.-Q. Li, P. Cui, R.-X. Xu, and Y. Yan, "Dynamics of quantum dissipation systems interacting with fermion and boson grand canonical bath ensembles: Hierarchical equations of motion approach," J. Chem. Phys. 126,
- 94 A. Ghosh, S. S. Sinha, and D. S. Ray, "Canonical formulation of quantum dissipation and noise in a generalized spin bath," Phys. Rev. E 86, 011122 (2012).
- 95 A. Riera-Campeny, A. Sanpera, and P. Strasberg, "Quantum systems correlated with a finite bath: Nonequilibrium dynamics and thermodynamics," PRX Quantum 2, 010340 (2021).
- $^{96}$ J. E. Runeson and J. O. Richardson, "Generalized spin mapping for quantumclassical dynamics," J. Chem. Phys. 152, 084110 (2020).
- 97 D. Bossion, W. Ying, S. N. Chowdhury, and P. Huo, "Non-adiabatic mapping dynamics in the phase space of the SU(N) lie group," J. Chem. Phys. 157, 084105
- $^{\bf 98}$  J. Schwinger, L. C. Biedenharn, and H. Van Dam, in  $\it Quantum\ Theory\ of\ Angular$ Momentum (Academic, New York, 1965); See also J. J. Sakurai, Modern Quantum Mechanics (Addison-Wesley, New York, 1994), p. 217.
- 99 For Ohmic spectral density function shown in Eq. (27), the real part of TCF, which is temperature-independent, reads as

$$\operatorname{Re}[C(t)] = \frac{\alpha \omega_c^2 (1 - \omega_c^2 t^2)}{2(1 + \omega_c^2 t^2)^2}.$$

At zero temperature, the imaginary part of the TCF has analytical expression [cf. Eq. (24b)],

$$\operatorname{Im}\left[C(t)\right]\big|_{T=0} = -\frac{\alpha\omega_c^3 t}{\left(1 + \omega_c^2 t^2\right)^2}.$$

100 K. D. Schotte, "On the spin fluctuation approach to the Anderson and Kondo Hamiltonians," Z. Phys. A 235, 155-165 (1970).